Cell Reports, Volume *29*

Supplemental Information

An Immunocompetent Mouse Model of HPV16(+) Head and Neck Squamous Cell Carcinoma

Miranda B. Carper, Scott Troutman, Bethany L. Wagner, Kevin M. Byrd, Sara R. Selitsky, Kshitij Parag-Sharma, Erin C. Henry, Weimin Li, Joel S. Parker, Stephanie A. Montgomery, John L. Cleveland, Scott E. Williams, Joseph L. Kissil, David N. Hayes, and Antonio L. Amelio

A

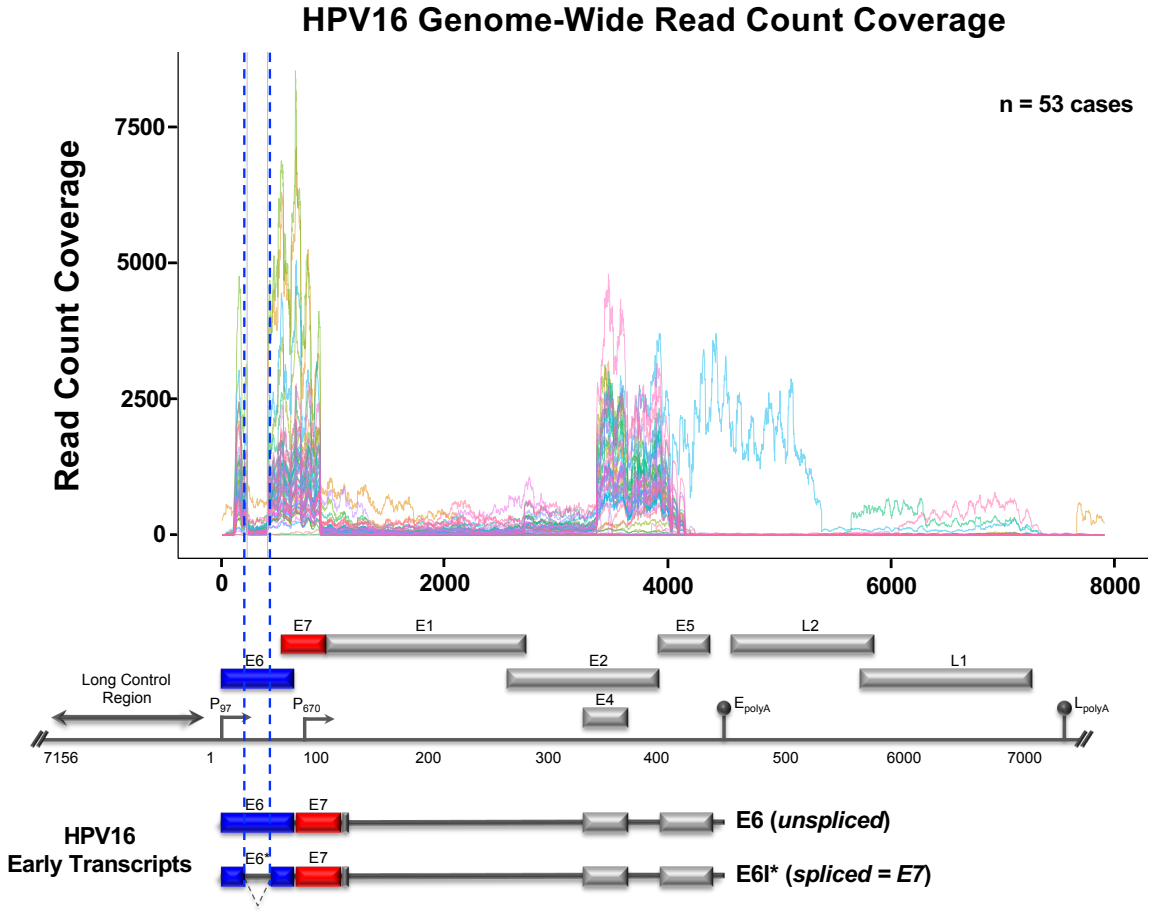

B

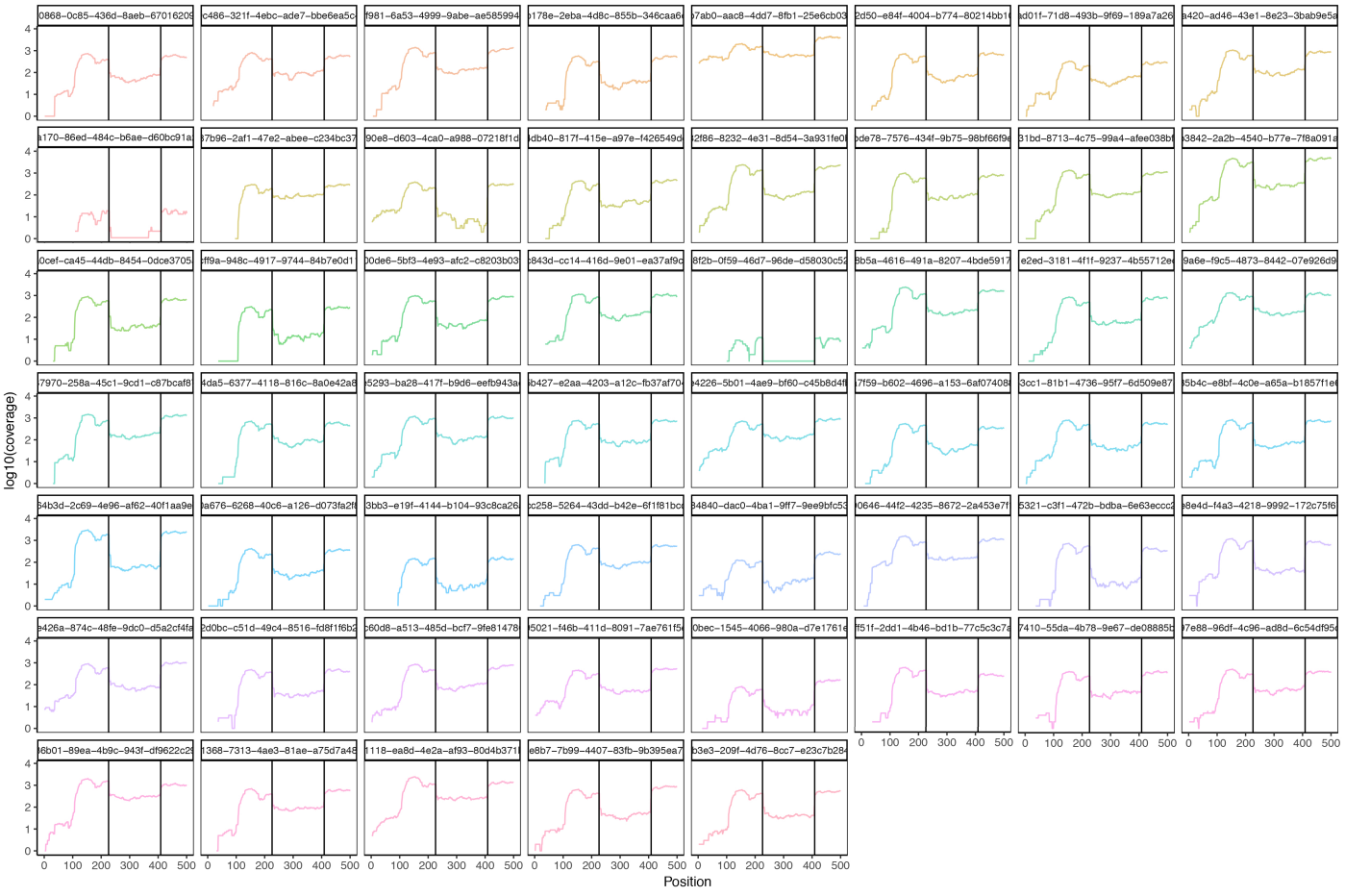

Supplemental Figure S1

Figure S1. HPV16 mRNA expression profiles in HNSCC map to early transcripts encoding E6 and E7. Related to Figure 1.

(**A**) Raw RNAseq read counts aligned to the PaVE database HPV16 reference genome. *Top*, raw read count coverage is graphed for HPV(+) HNSCC samples with median E6 (unspliced) coverage > 100.51 counts (n = 53). *Bottom*, illustration of the HPV16 genome with position of the early promoter indicated, boxes highlighting open reading frames for the E6 (blue) and E7 (red) oncogenes, and select alternatively spliced HPV16 mRNAs translated to E6 or E7.

(**B**) Log10 (raw read counts) aligned to HPV16 genome from position 0 to 500 were used to discriminate between unspliced E6 and alternatively spliced E6*I (translated to E7) transcripts. Solid black lines represent the splice junction at position 227 and 408. Each HPV(+) HNSCC sample is plotted in a separate panel. Plots shown for selected HPV(+) samples were used to analyze the ratio between the mean of mapped reads flanking unspliced sequences (nt 226-227 and 408-409) versus the mean of mapped reads spanning the alternatively spliced region (nt 226^409).

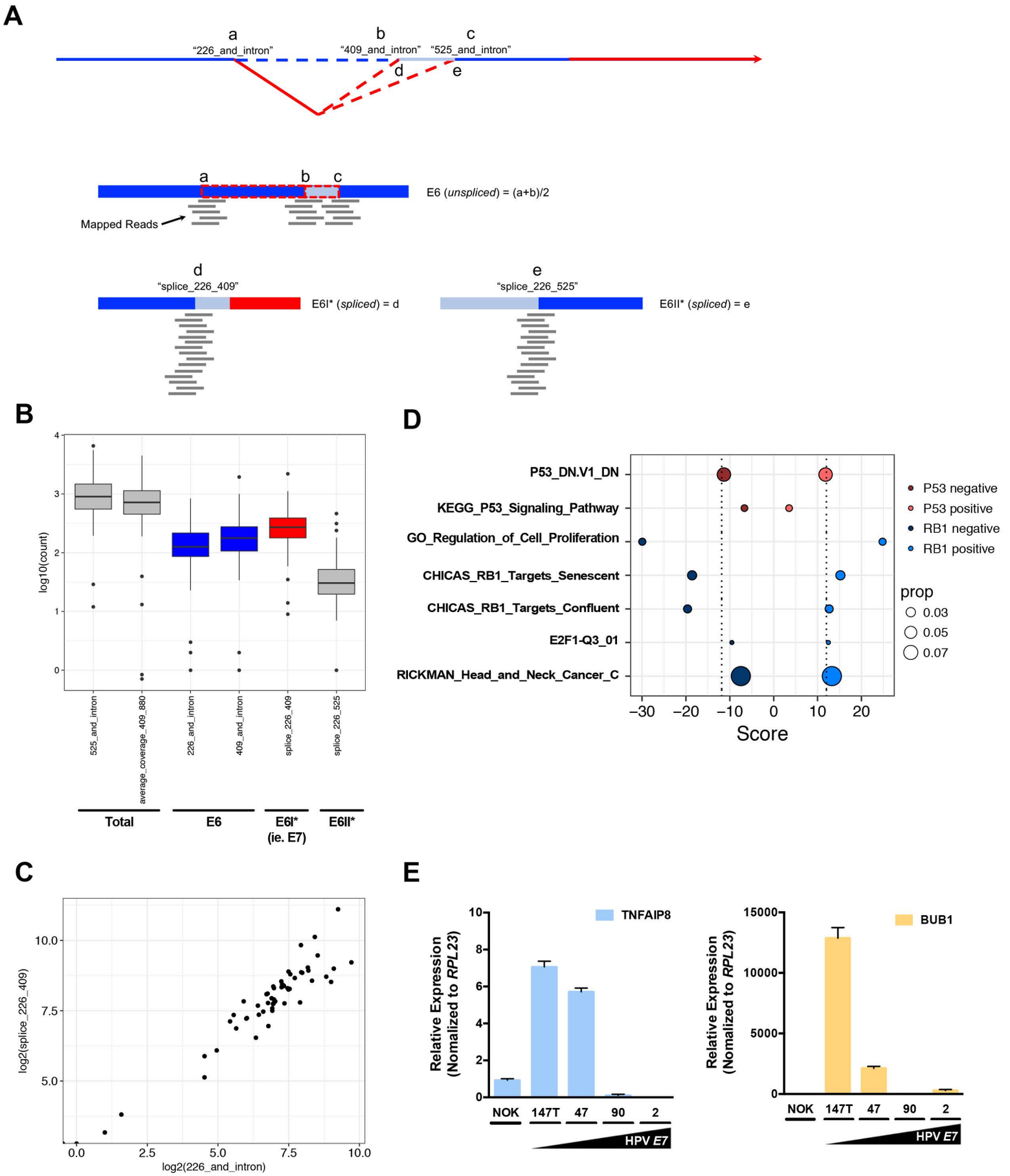

Supplemental Figure S2

Figure S2. Bioinformatics analysis reveals near 1:1 E6/E7 stoichiometry in HPV(+) HNSCC and expected deregulation of E6/TP53 and E7/E2F1 pathways. Related to Figure 1.

(**A**) Schematic of alternatively spliced HPV16 early transcripts encoding E6 and E7.

(**B**) Box and whisker plot of the log10 transformed raw read counts of total and alternatively spliced HPV16 early transcripts.

(**C**) Spearman's rank correlation coefficient of expression levels (log2 raw read counts) for spliced E6I* (E7) versus unspliced (E6) HPV16 early transcripts ($\rho = 0.9149$).

(**D**) Gene set enrichment analysis (GSEA) of E6/TP53 and E7/E2F1 pathway genes. Size of the circles in the bubble plot is the proportion to the number of genes within each pathway that are statistically significant (adjusted p-value < 0.05). The hatched lines reflect q-score = 0.05.

(**E**) Real-time qPCR analysis of select E6/p53 host pathway genes in HPV positive HNSCC cell lines relative to control HPV negative NOK cells. Relative fold expression is shown normalized to *RPL23* mRNA levels ($n = 3$, mean±SEM).

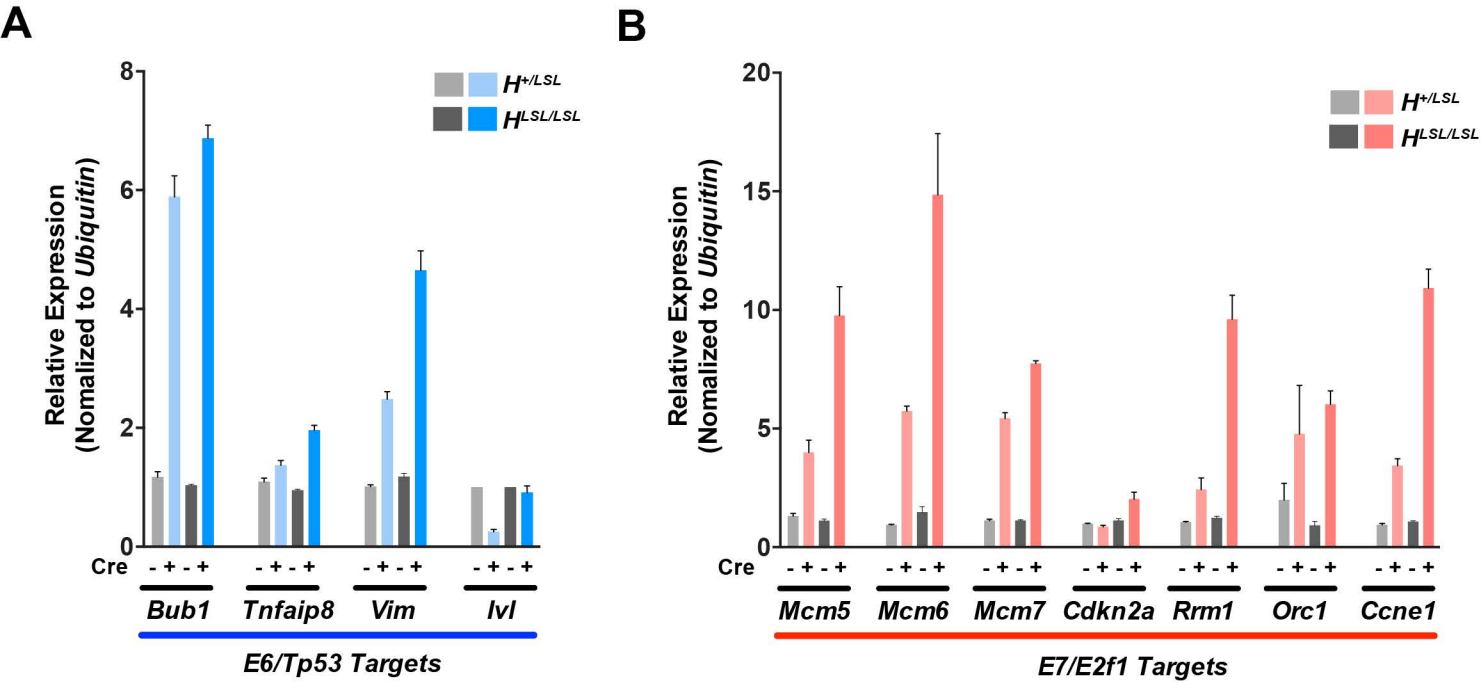

Supplemental Figure S3

Figure S3. Modulation of E6/Tp53 and E7/E2f1 target genes involved in cell cycle, proliferation, differentiation, and mobility. Related to Figure 2.

(**A**) Real-time qPCR analysis of common E6/Tp53 target genes in $H^{+/LSL}$ or $H^{LSL/LSL}$ MEFs transduced with either GFP or Cre adenoviruses. Relative fold expression is shown normalized to *Ubb* mRNA levels (n = 3, mean±SEM).

(**B**) Real-time qPCR analysis of common E7/E2F1 target genes in $H^{+/LSL}$ or $H^{LSL/LSL}$ MEFs transduced with either GFP or Cre adenoviruses. Relative fold expression is shown normalized to *Ubb* mRNA levels (n = 3, mean±SEM).

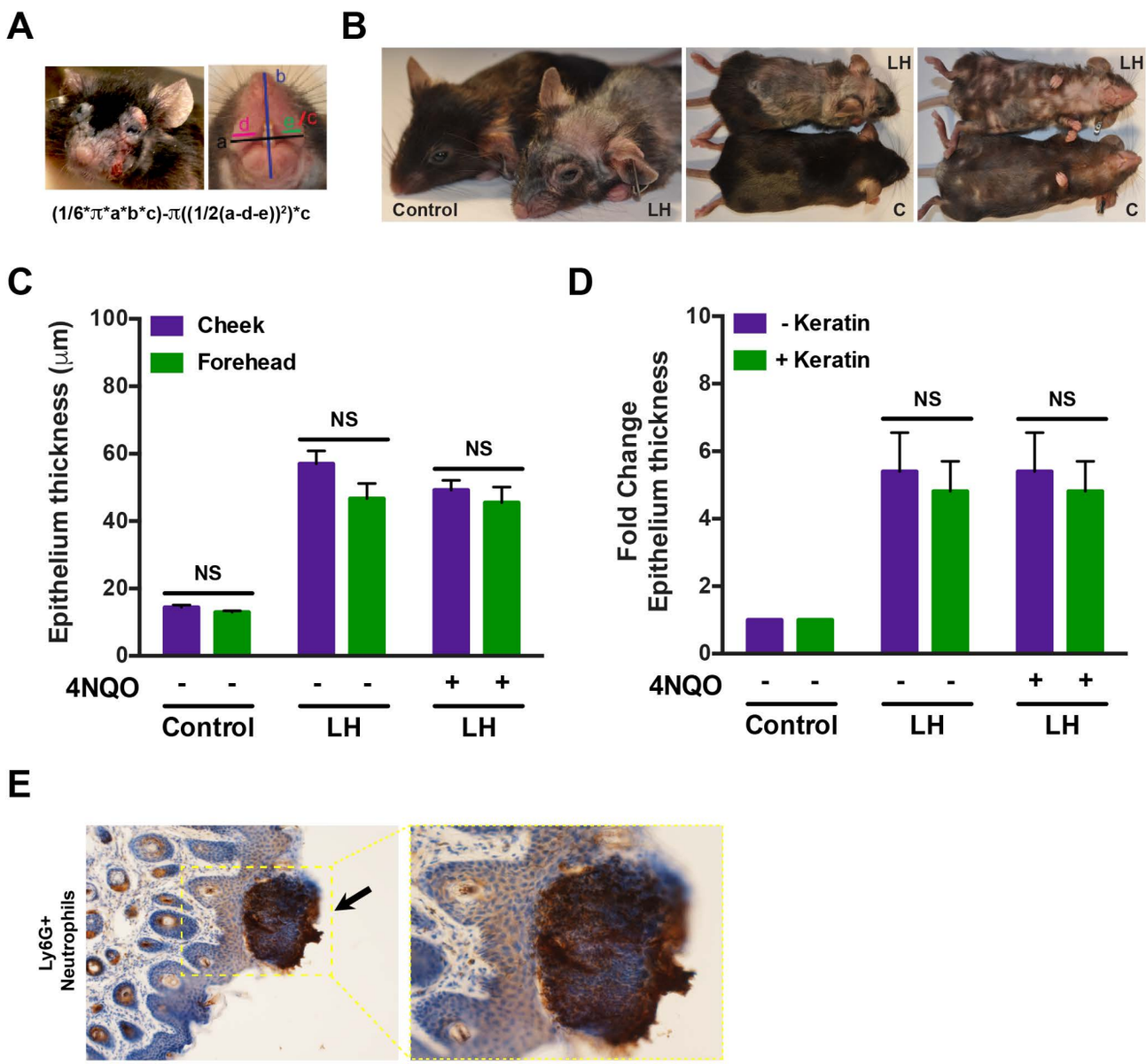

Supplemental Figure S4

Figure S4. Low-dose 4NQO treatment does not impact epithelium thickness or enhance tongue tumorigenesis in LH mice. Related to Figure 3.

(**A**) Representative image of late-stage LH animal (> p365 days), *left*. Formula used for calculating oral volumes as described in Zhong, R et al. (2014). *Can Res*. Orthogonal dimensions a (black line), b (blue line), and c (red line) are indicated and used for measuring ellipsoid volume while d (red line) and e (green line) are used for measuring the cylindrically shaped oral aperture.

(**B**) Representative dorsal and ventral photographs of control littermates and the LH animals treated with low-dose 4NQO (20 μg/ml) in the drinking water for 8 weeks followed by weekly oral cavity examination for gross pathologic changes.

(**C**) Anatomic location of face skin does not influence epithelium thickness in LH mice. Quantification of the average epithelium thickness for cheek and forehead face skin in control littermate or LH mice treated +/- 4NQO (20 μg/ml).

(**D**) Comparison of epidermal thickness measurements +/- keratin layer. Quantification of epithelium thickness +/- keratin in forehead face skin does not impact average fold in control littermate or LH mice treated +/- 4NQO (20 μg/ml).

(**E**) Immunohistochemical analysis of immune cell infiltration. Representative sections from adult cutaneous epithelia were formalin fixed, embedded, and stained for Ly6g+ neutrophils. Magnification = 100x, Bar = 200 μm (Inset = 200x).

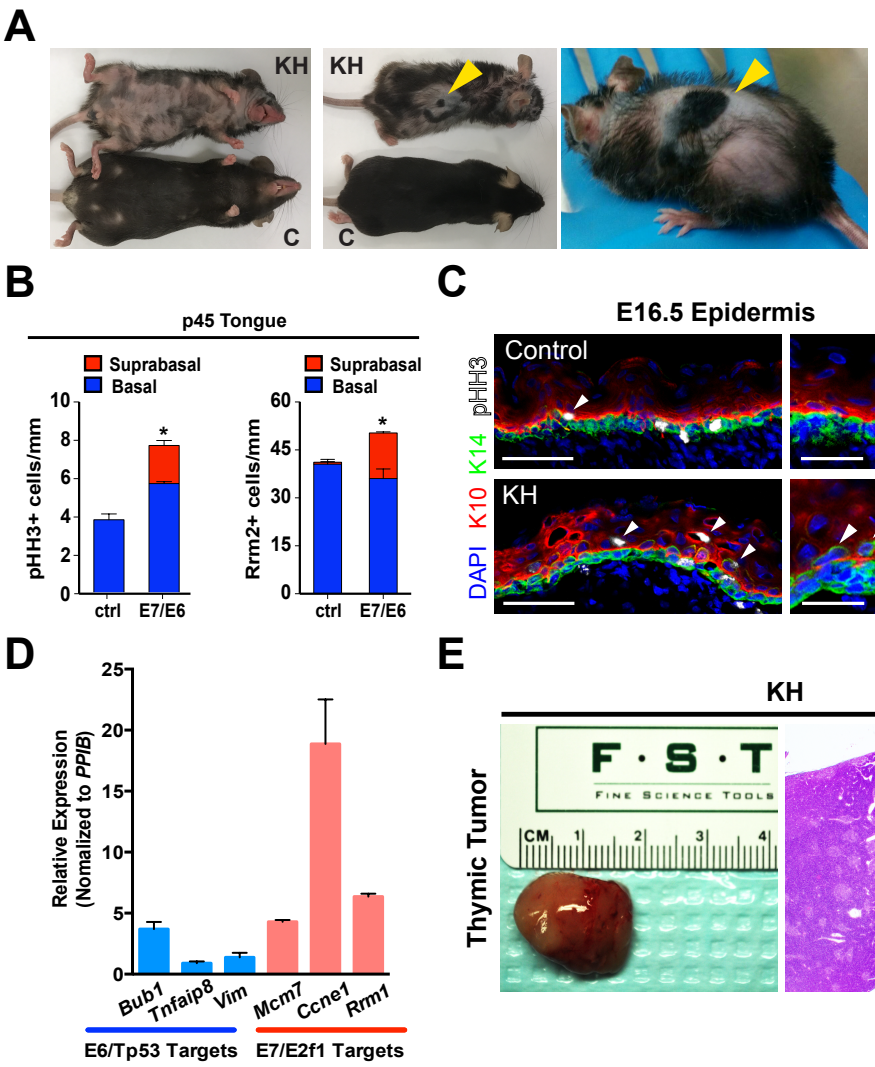

Supplemental Figure S5

Figure S5. HPV16 E6 and E7 expression within stem cell compartments of the skin disrupts normal developmental processes. Related to Figure 4.

(**A**) Representative dorsal and ventral photographs of control littermates and KH animals. Yellow arrowheads denote observed disruption in hair follicle homeostasis.

(**B**) Mitotic defects in epithelial cells expressing E7/E2f1 target genes. Quantification of mitotic rates in adult p45 KH tongues (*left*) and the E7/E2f1 target Rrm2 (*right*). Overall mitotic rates are increased in HPV(+) tissues, accompanied by a significant increase in suprabasal mitoses (red).

(**C**) Mitotic defects are evident in embryonic tissues. *Left*, E16.5 epidermis from KH and control embryos showing expression of the basal marker K14 (green), spinous marker K10 (red) and mitotic cells (pHH3, white). White arrowheads indicate suprabasal mitoses occurring outside the basal layer. *Right*, high magnification images showing ectopic K14+ cells (white arrowheads) that occur in E7/E6+ epidermis. Magnification = 400x, Bar = 50 μm. Note also how spinous cells in the E7/E6 epidermis have round nuclei, in contrast to the normal flattened cells in controls.

(**D**) Real-time qPCR analysis of select E6/Tp53 and E7/E2F1 host pathway genes in neonatal (p0) KH and control littermate mice. Relative fold expression is shown normalized to *Ppib* mRNA levels ($n = 3$, mean±SEM).

(**E**) Histologic analysis of representative thymic epithelial tumors. Macroscopic images of thymic tumors derived from adult KH mice, left. H&E stained thymic tumor section submitted for histopathological examination. Magnification = 200x, Bar = 200 μm.

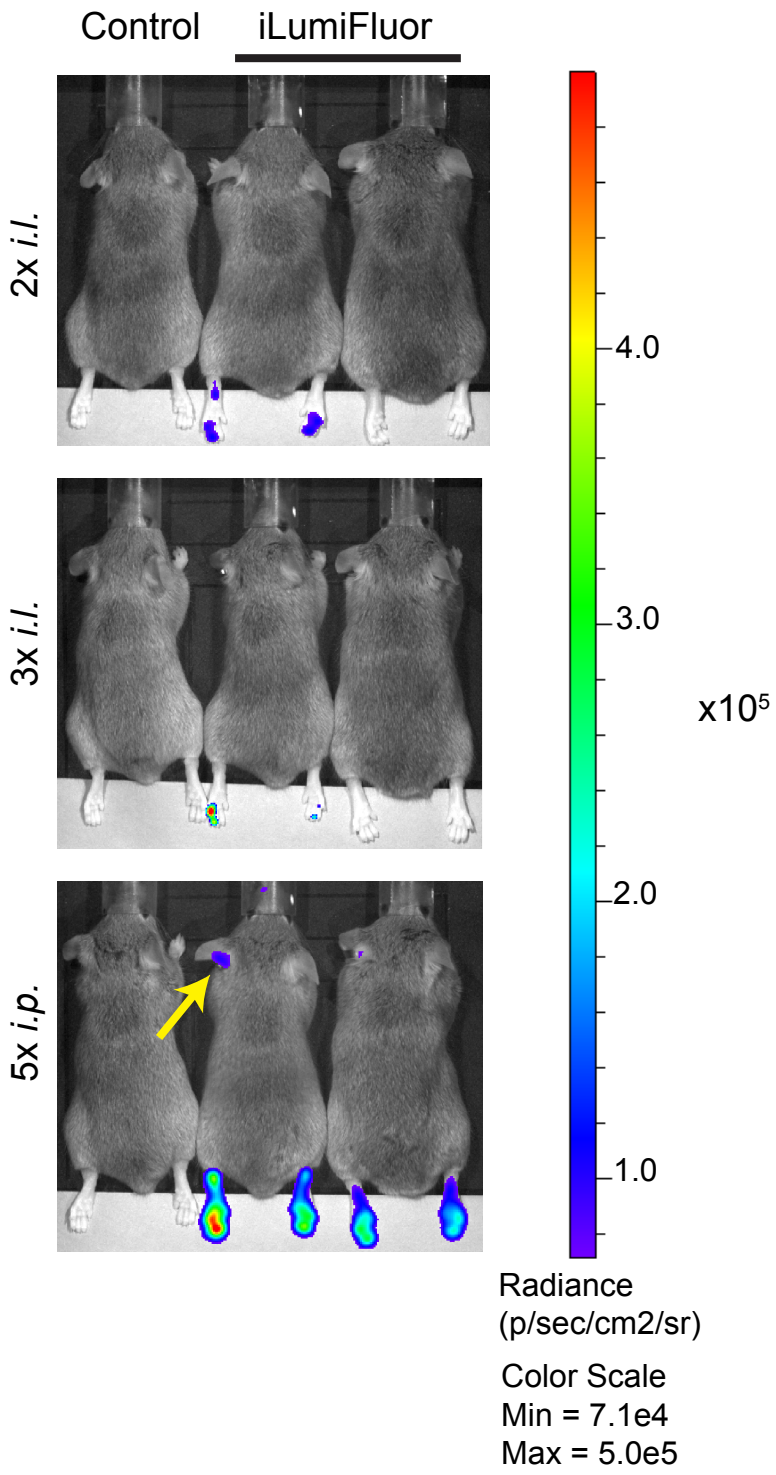

Supplemental Figure S6

Figure S6. Targeted *intra*-lingual TAM administration minimizes global epithelial activation. Related to Figure 5.

Representative BLI images of iLumiFluor and control littermates comparing TAM dose and delivery (*i.l.* versus *i.p.*) 10 days following last TAM injection. Animals administered TAM 5x *i.p.* displayed increased bioluminescent signals in off-target, non-fur bearing tissues (n = 5).

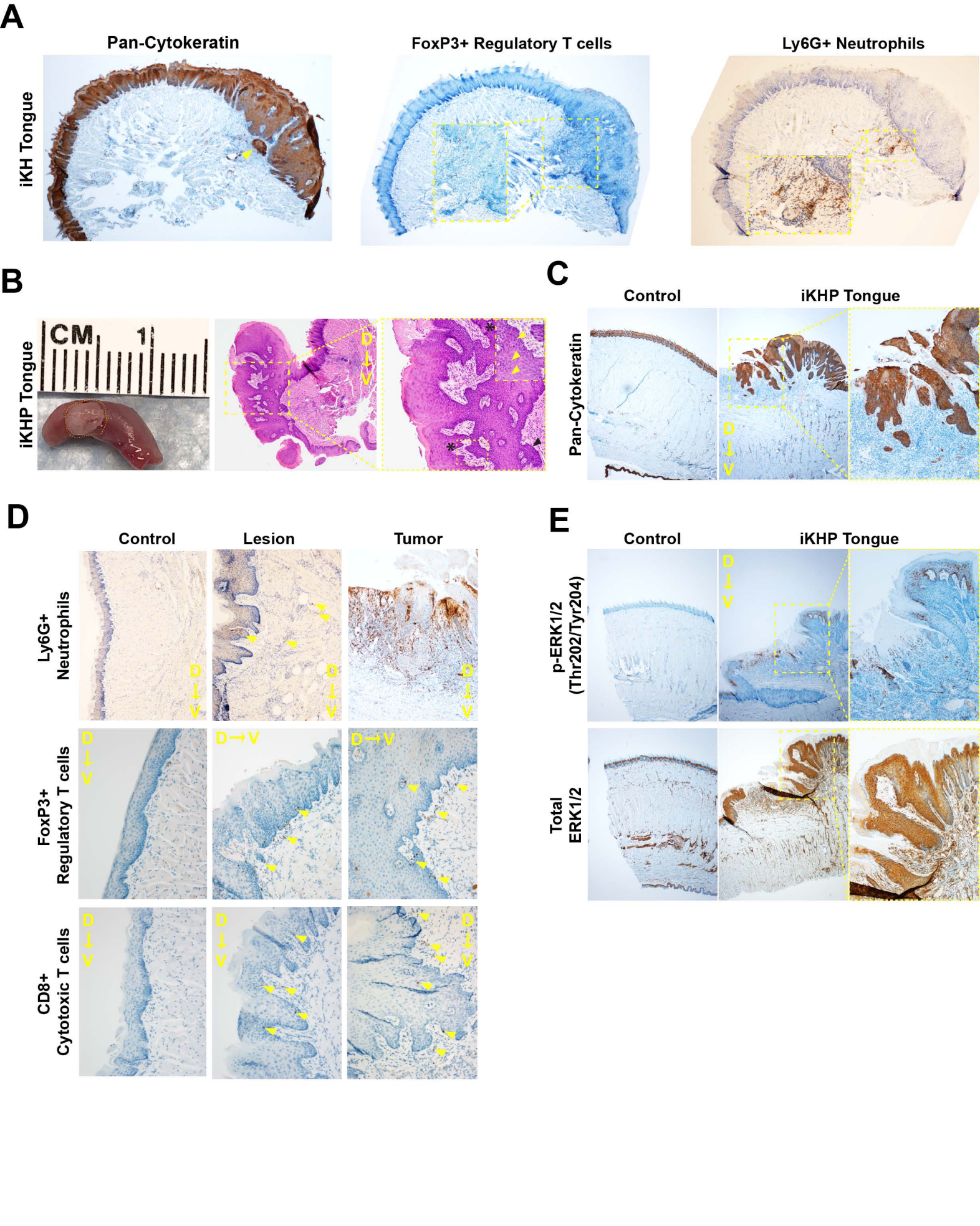

Supplemental Figure S7

Figure S7. Phenotypic characterization of tumors and immune cell infiltrates. Related to Figures 6 and 7.

(**A**) Representative sections from formalin fixed, embedded, and stained iKH tongues reveal morphologic and histologic abnormalities consistent with oropharyngeal squamous cell carcinoma. Immunohistochemistry (IHC) staining for pan-cytokeratin (*left*), FoxP3+ regulatory T cells (*middle*), and Ly6g+ neutrophils (*right*). Magnification = 40x, Bar = 200 μm (Inset = 100x).

(**B**) Mutant PIK3CA cooperates with HPV16 E6 and E7 oncogenes to drive tumorigenesis. *Left*, representative image of the gross morphology and H&E stained sections for a moderately differentiated iKHP tongue tumor (6-8 weeks). Tumor inset highlights invasive features (*right,* 100x) including basement membrane disruption with muscle invasion (black arrowhead) and mitotic figures (*asterisk,* 600x - yellow arrowheads). Magnification (*left*) = 40x, Bar = 200 μm.

(**C**) Representative immunohistochemistry (IHC) of sections from formalin fixed, embedded, and stained for pan-cytokeratin iKHP versus control tongues reveal morphologic and histologic abnormalities consistent with oropharyngeal squamous cell carcinoma. Magnification = 40x, Bar = 200 μm (Inset = 100x).

(**D**) IHC analysis of immune cell infiltration. representative sections of control tongues compared to iKHP tongues harboring early, pre-malignant lesions (4-6 weeks) or tumors (6-8 weeks) stained for Ly6g+ neutrophils (*top*), FoxP3+ regulatory T cells (*middle*), or Cd8+ cytotoxic T cells (*bottom*). Magnification = 40x, Bar = 200 μm (Inset = 100x).

(**E**) Representative IHC staining of total ERK1/2 demonstrating suprabasal expression in control and iKHP tumors (*bottom*) but only modest p-ERK1/2$^{Thr202/Tyr204}$ (*top*) staining. Magnification = 400x, Bar = 200 μm (Inset = 100x).